General Sensitivity Analysis of Solar Thermal-Electric Plants

F. L. Lansing, E. W. Hayes, and C. S. Yung
DSN Engineering Section

Performance optimization of solar thermal-electric power systems depends on a number of major parameters, each affecting the specific power output and the overall conversion efficiency differently in magnitude and direction. This first-phase study presents analytically a unified and generalized treatment in predicting the technical performance of many present or future system designs and configurations. In an effort to screen the major design parameters whose effect on performance is high and to assess the system improvement or deficiency resulting from their change, the sensitivity analysis is performed. The sensitivity, defined as the percentage change of output divided by the percentage change in input, is evaluated analytically for seven major system design parameters. These design parameters are: the solar radiation intensity, the ambient temperature, the optical-thermal characteristics of the collector subsystem (concentrator-receiver), the relative thermal efficiency for the energy conversion subsystem, the working fluid operating temperature, and the rate of fluid heat capacity. General performance sensitivity expressions are derived and numerically evaluated for the range of possible operating conditions. Furthermore, the effect of these major parameters on the system performance optimization is presented to identify future improvement areas and to pave the way for the second-phase study in the economic sensitivity analysis on bus bar energy costs.

I. Introduction

To satisfy the NASA goals of facilities energy conservation and the nationwide energy self-independence program, the Deep Space Network (DSN) is studying, among others, the concept of installing a 1-10 MW(e) solar thermal-electric power plant at one of its three deep space communications complexes.

Of major concern in the design of such a solar-powered plant is the need for insolation data, load profiles, weather data and the specification of some minimum, average or peak values for the major design parameters. These design parameters, and environment data, will have errors either small or large when first estimated or measured. Moreover, it is expected that the actual operation of the power plant will be fluctuating and intermittent with interruptions depending on solar energy fluctuations, load variations, storage capacities, and its automatic control strategy, and, therefore, the actual plant operation will be different from what is designed. The deviation or discrepancy between design and actual operation could result in either serious or negligible effects (depending on the design parameter) on the overall plant performance. The serious effects will affect the estimated cost of the electrical energy produced at the bus bar.

An interesting attempt to investigate the sensitivity of solar thermal-electric output to the dynamics of the solar radiation was presented in Refs. 1 and 2. In this dynamic model, sinusoids of different wavelength and frequency are imposed to simulate the solar transients on two different types of energy collection subsystems – a slow response and a fast response type, coupled with a reversible power conversion cycle. The results of Refs. 1 and 2 are later discussed and verified in this work. However, since they are focused only on the variations of solar intensities, more work is felt needed to evaluate the sensitivity to other major design parameters.

This article presents, in a generalized way, the first part of the study which is to assess the consequences of the errors or design differences on the technical performance of the whole system. The objectives are to give an indication of the levels of tolerance which are acceptable, to shed some light onto the weight of each design parameter, and to seek ways to optimize the performance.

Some parts of the present study are described in simple and unsophisticated fashion in order to be transmitted to a wide range of reader backgrounds including those with limited experience in solar energy. Numerous papers in the literature have addressed in more detail the performance of various subsystems or components of many possible solar-plant configurations. The present study is not intended to review the technical performance of the individual component but, rather, cover the whole system behavior to enable the sensitivity analysis to be made.

One of the most important parameters that needs to be considered in the sensitivity analysis is the bus bar energy cost. This cost, besides its dependence on average annual performance and the total electrical energy produced over the lifetime of the plant, depends on the life cycle costs, including the installation costs, inflation rates, interest rates, taxes, depreciation, maintenance costs, etc., which require continuous updating from existing solar plants.

Although the present first-phase study gives the consequences of only the design parameters of differences on performance, the methodology followed can and will be extended in the future to cover the economic parameters as well as the design parameters. The temporary elimination of the bus bar energy cost from the technical analysis is assumed in this study not to cause a change of the point at which the overall system economics are optimum.

II. General Analysis

All conceivable present and future solar thermal power plants could be treated as a combination of the following subsystems: (1) an energy collection subsystem including the reflecting and absorbing surfaces, concentrators, and receivers through which the sun's light energy is converted into thermal energy as a sensible or latent heat carried away by a working fluid; (2) an energy conversion subsystem which is following an advanced power cycle including heat exchangers for heat addition, rejection, and regeneration; (3) an energy storage subsystem which matches the supply (solar energy) with the demand (electrical connected loads); and (4) an energy transmission subsystem to transmit the energy (in either thermal, chemical, or electrical form) from one subsystem to another.

The present sensitivity study is performed with the above solar system under consideration treated as a sequence of steady rate processes in subsystems held at a steady or quasi-steady state, i.e., no transient dynamics or intermittent operation is allowed. To illustrate this condition futher, consider as in Fig. 1 a solar thermal-electric power plant which is supplying an electrical load only at night time through an energy storage subsystem. The storage subsystem is charged in the sunny hours and is discharged at night. If the instantaneous plant efficiency is defined as the ratio between the electrical-connected loads and the incident solar energy, then the efficiency sensitivity to diurnal solar flux variations will be zero in the sunny period and infinity during the night period. The study, therefore, will have no value if intermittent or transient conditions prevail, since the term "efficiency" becomes meaningless. Therefore, we will proceed only under the conditions of steady or "quasi"-steady state. The treatment of storage systems and transient dynamics requires integrating or time-averaging techniques which require more information about the solar load profiles.

The installation cost of a solar-electric power plant and the bus bar unit energy cost are greatly influenced by the overall conversion efficiency. When the energy conversion is done via thermal power cycles, the overall efficiency becomes the product of collection efficiency, power cycle thermal efficiency, energy through storage efficiency, and energy transmission efficiencies.

The efficiency trends pertain to all collectors, and power cycles could, in general, be formulated as follows. The collection efficiency always decreases with increasing fluid operating temperature due to higher thermal losses and could reach zero when the incident solar radiation equals these losses. The power cycle efficiency, on the other hand, increases monotonically with the operating temperature and starts from zero at ambient temperature, as shown in Fig. 2. The overall conversion efficiency will be zero at both ends I and II of Fig. 2, and always possesses a maximum value in between them. For a good design, the optimum operating temperature T_c^* corresponding to the maximum overall conversion efficiency, η_0^*, should be the system design point. Although a minimization of the bus bar energy cost may or may not require the operation at the peak plant efficiency, we will assume, for the present discussion, that the peak conversion efficiency is the desired goal.

The performance of solar collectors is generally the same whether they are focusing or nonfocusing types. The instantaneous efficiency of the collection subsystem could be, in general, approximated by a linear form similar to the Bliss, Whillier, and Hottel form:

$$\eta_c = A - B(T_c - T_a)/I \tag{1}$$

where A and B are characteristic constants which depend on the material optical properties, collector geometry, heat losses, and fluid flow characteristics, T_c is the inlet fluid temperature, T_a is the ambient temperature, and I is the total solar flux. This linear form can be used as a piecewise approximation in the range of interest in the performance of high concentration collectors operating at high temperatures. For these cases, the efficiency trends are concave bending downward due to the effect of IR radiation losses, which are proportional to temperatures to the power 4. By proper choice of the constants A and B, the linear expression could provide a good approximation over the working range.

From an energy balance viewpoint, the collection efficiency, η_c, can also be expressed equivalently as

$$\eta_c = G_f C_f (T_H - T_c)/I \tag{2}$$

where G_f and C_f are the fluid mass flux and specific heat, respectively, and T_H is the exit fluid temperature. Equation (1) contains two collector-specific constants which are derived using the physical and optical properties through either theoretical analyses or by experiment. The exit fluid temperature, T_H, is completely omitted from Eq. (1), but could be obtained from Eq. (2). The constant A is proportional to the product of optical transmissivity or reflectivity and receiver absorptivity. The second term in Eq. (1) represents approximately how much heat is lost to the atmosphere, and the difference represents the net solar energy fraction collected by the transfer fluid. The collector efficiency, therefore, can be negative or positive depending on the fluid temperature at the collector entrance. Equation (1) is selected for the present general sensitivity analysis because the variables it contains are independent of each other and, in general, is a simple representation of many conceivable collectors (Refs. 3-14).

The second step is to determine an efficiency expression for the energy conversion subsystem. To treat the problem, also in a general way, let us assume that the power cycle under consideration performs as a percentage of the efficiency of a reversible Carnot cycle operating between the hot finite heat reservoir (fluid) and the cold infinite heat reservoir (ambient).

Using the laws of available and unavailable work in thermodynamics when working between these two heat reservoirs, the reversible work obtainable can be written for a constant specific heat fluid as

$$W_{\text{rev}} = G_f C_f (T_H - T_c) - G_f C_f T_a \ln (T_H/T_c)$$

The expression for the reversible cycle efficiency becomes

$$\eta_e = 1 - \frac{T_a \ln (T_H/T_c)}{(T_H - T_c)} \tag{3}$$

The efficiency in Eq. (3) is more adequate than the Carnot's expression for two infinite heat reservoirs $(1 - T_a/T_H)$; besides that, it is applicable to any thermodynamic cycle operating between the above temperature limits (T_c, T_H, and T_a).

The third step in the general analysis is to develop an expression for the overall solar-electric efficiency to be entirely made of independent system variables. The fraction λ, the efficiency ratio of a real power cycle as compared with a reversible one, is a design characteristic of the energy conversion subsystem. For simplicity, the fraction λ could be assumed to embody the energy storage and transmission efficiencies as well. The outlet temperature of the collector fluid, as required in solving Eq. (3), could be expressed in terms of independent variables by setting Eqs. (1) and (2) equal when assuming negligible temperature drop in the energy transmission lines. Hence,

$$T_H = T_c + \left[A - B\left(\frac{T_c - T_a}{I}\right)\right]\frac{I}{G_f C_f} \tag{4}$$

The final expression for the system overall efficiency (η_0) is the product of collection and conversion efficiencies, which is written as

$$\eta_0 = \eta_c \, \eta_e \, \lambda \tag{5}$$

The expressions in Eqs. (1) through (5) simplify the performance of all solar thermal-electric power plants and lead to the general sensitivity analysis presented next.

III. Sensitivity Relations

The sensitivity concept is beneficial to the designer in allowing to sense in both magnitude and direction the effect of small or large deviations occurring in the various design parameters on the performance of the solar power plant. The sensitivity is the measure of the dependency of system characteristics on variations occurring in a particular element or parameter, as shown in Fig. 3. The sensitivity(s) is expressed analytically as:

$$S = \left(\frac{\Delta Y/Y}{\Delta X/X}\right)_r$$

or

$$S = \left(\frac{dY}{dX}\cdot\frac{X}{Y}\right)_r \tag{6}$$

or

$$S = \left(\frac{d\ln Y}{d\ln X}\right)_r$$

where X is an arbitrary input element, Y is the system output, Δ represents a differential change in either X or Y, and the subscript (r) denotes conditions at a reference point. Equation (6) states that the differential sensitivity of Y with respect to X is the percentage change in Y divided by that percentage change in X which caused the change in Y to occur, keeping all other input elements unchanged. The definition is suitable only for small changes. Any system operating at an optimum value of one of its elements should have zero sensitivity with respect to this element.

The concept of sensitivity has been widely used in studying automatic controls, electric circuits, and many physical systems, and its present application to solar power plants represents a useful tool in the performance optimization.

In solar power plants, the input element X could be any one of the following:

(1) Inlet fluid temperature to the energy collection subsystem (T_c).

(2) Collector optical characteristic constant, A.

(3) Collector thermal characteristic constant, B.

(4) Ambient temperature, T_a.

(5) Incident solar flux, I.

(6) Heat capacity of collector fluid, $G_f C_f$.

(7) Relative efficiency of energy conversion and transmission subsystems, λ.

Note that the exit fluid temperature T_H could be expressed in terms of the other independent parameters in Eq. (4).

The system output, Y, on the other hand, could be: (1) the overall solar-electric conversion efficiency, η_0, (2) the net electrical (or mechanical) work output per unit collector W, where

$$W = \eta_0 I \tag{7}$$

or (3) the unit energy cost at the bus bar. Only the first two output variables are selected in this study. The sensitivity of the overall conversion efficiency to any input parameter X is denoted by S_x and that of the net electrical (or mechanical) work output to the input parameter X by $\bar{S}_x$. It can be easily proven from Eqs. (5), (6), and (7) that at a reference state (r),

$$S_x = \left[\frac{X}{\eta_0}\left(\frac{\partial \eta_0}{\partial X}\right)\right]_r$$

or

$$S_x = \left[\frac{X}{\eta_c}\left(\frac{\partial \eta_c}{\partial X}\right) + \frac{X}{\eta_e}\left(\frac{\partial \eta_e}{\partial X}\right) + \frac{X}{\lambda}\left(\frac{\partial \lambda}{\partial X}\right)\right]_r \tag{8}$$

and

$$\bar{S}_x = \left[\frac{X}{W}\left(\frac{\partial W}{\partial X}\right)\right]_r \tag{9a}$$

and using Eqs. (7) and (8),

$$\bar{S}_x = S_x + \left[\frac{X}{I}\left(\frac{\partial I}{\partial X}\right)\right]_r \tag{9b}$$

Also, it can be seen that if the overall efficiency (η_0) is written as $\eta_0(X_1, X_2, \ldots)$, then

$$\left(\frac{\Delta\eta_0}{\eta_0}\right) = S_{X_1}\left(\frac{\Delta X_1}{X_1}\right) + S_{X_2}\left(\frac{\Delta X_2}{X_2}\right) + \cdots \tag{10}$$

where X_1, X_2 are input parameters. Equation (10) is very important in determining the total effect of all input parameters of the system when each varies in magnitude and direction differently throughout the operating time.

The sensitivity expressions for each parameter have been derived following Eqs. (8) and (9) and simplified by algebraic manipulations of Eqs. (1) through (4). The results are discussed next.

IV. Results of Parameter Variations

All parameters used in the sensitivity analysis are given in standard international (SI) units. The values and ranges for each parameter were chosen from the practice gained in operating 12 different collector types (Refs. 3-14). Each solar collector has, as an approximate representation, two identifying design parameters, namely, A and B, as shown in Fig. 4. For low concentration collectors, with a concentration ratio of 1-5, the B values range from 0.0030 to 0.0060 kW/m^2°C and the A values range from 0.4 to 0.8; for high concentration collectors, with a concentration ratio above 100:1,[1] the value of A ranges from 0.6 to 0.9 and B ranges from 0.0001 to 0.0010 kW/m^2°C (Ref. 12). The fluid heat capacity ($G_f C_f$) may range from 0.01 to 0.05 kW/m^2°C depending on the required temperature rise and the trade-off between pumping power and system efficiency. A nominal flow heat flux of 0.04 kW/m^2°C is selected as a reference point only for the next discussion. As a reference weather, the ambient temperature is taken as 25°C (77°F), and the nominal solar flux is taken as 1 kW/m^2 (1 sun).

The relative efficiency of the energy conversion-transmission subsystem compared to the reversible path usually ranges from 40 to 60 percent and a value of 50 percent was chosen arbitrarily in the reference operating conditions.

A. Sensitivity to Inlet Fluid Temperature

The sensitivity of the overall efficiency to changes in the collector's inlet fluid temperature can be derived from Eqs. (8) and (9). After performing the differentiation, the sensitivity expression is reduced to

$$\bar{S}_{T_c} = S_{T_c} = \frac{T_a(AI + BT_a) - B\,T_c T_H}{\eta_e \eta_c I T_H} \qquad (11)$$

The sensitivity S_{T_c} could be negative, zero or positive, depending on whether the inlet fluid temperature T_c is smaller than, equal to, or larger than the optimum temperature T_c^*, respectively. The optimum inlet fluid temperature, T_c^*, is the temperature at which the overall efficiency is a maximum, or at which the sensitivity S_{T_c} is zero. In the special case where the flow rate is such that the temperature difference across the collector (between inlet and exit fluid temperatures) is small, i.e., $T_c \sim T_H$, then the optimum fluid temperature T_c^* can be given from Eq. (11) approximately as

$$T_c^* \cong \sqrt{T_a^2 + \frac{AIT_a}{B}} \qquad (12a)$$

[1]Concentration ratio of parabolic dishes could range from 1500 to 2000.

Accordingly, the reversible cycle efficiency in Eq. (3) becomes

$$\eta_e^* \cong 1 - \frac{T_a}{T_c^*} \qquad (12b)$$

In general, a more accurate, but somewhat complex, expression for T_c^* could be derived from Eq. (11) by substituting the exit fluid temperature, T_H^*, using Eq. (4). By solving the final quadratic equation, the expression for T_c^* in terms of the independent input parameters A, B, I, T_a and $G_f C_f$ becomes

$$T_c^* = \frac{(AI + BT_a)}{2(G_f C_f - B)} \left\{ \sqrt{1 + \frac{4 G_f C_f T_a (G_f C_f - B)}{B(AI + BT_a)}} - 1 \right\} \qquad (13)$$

It is interesting to know that Eq. (13) is independent of λ. The difference between the approximate expression of T_c^* in Eq. (12a) and the accurate one in Eq. (13) could be assessed by the following example. Suppose that the characteristic constants A and B for a given collector are 0.8 and 0.0057 kW/m^2°C, respectively, and that the fluid heat capacity $G_f C_f$ is 0.04 kW/m^2°C. With an ambient temperature of 25°C (298.15 K) and a solar intensity of 1 kW/m^2, the optimum temperature T_c^* from Eq. (12a) is 88.43°C (371.58 K) and that from Eq. (13) is 82.58°C (355.73 K), which shows their small difference. At the optimum inlet fluid temperature of 82.58°C, the optimum collector and reversible cycle efficiencies become 47.18 and 17.55 percent, respectively. Accordingly, if a real engine with a 50 percent relative efficiency is used, the maximum overall conversion efficiency for the system will be 4.14 percent, which is typical of high performance flat-plate collectors.

Hereafter, the above optimum inlet fluid temperature T_c^*, as determined from Eq. (13), which is assumed as the design point, will be adopted in our analysis as a fixed reference state at which the performance sensitivity is evaluated. This condition was imposed since solar-power plants should operate at their "best" conditions, and deviations from this optimum performance are what the sensitivity analysis is, in the first place, seeking to evaluate. Operation at any inlet fluid temperature other than T_c^* (either higher or lower) will always result in lower overall efficiency. In the above numerical example, for instance, if the operating inlet fluid temperature is lower than the optimum 82.58°C, by 10°C, say, the sensitivity S_{T_c} becomes 1.2972 and the overall efficiency becomes 4.06 percent. Therefore, operating at temperatures other than the optimum T_c^* will change the sensitivity S_{T_c}, as determined from Eq. (11), to be either positive or negative depending on whether $T_c < T_c^*$ or $T_c > T_c^*$, respectively. The maximum positive value of S_{T_c} occurs when the reversible cycle efficiency approaches zero, that is, when the temperatures T_c and T_H are close to the ambient T_a (see Fig.2), thus making S_{T_c} approaching infinity. On the other hand, the minimum value of S_{T_c} will be $-\infty$ when the temperature T_c theoretically reaches its limiting value $\bar{T}_c$. The latter is given from Eq. (1) by equating the collector efficiency to zero:

$$\bar{T}_c = T_a + \frac{AI}{B} \tag{14a}$$

Using the approximation made in Eq. (12a), then

$$\bar{T}_c \cong T_c^{*2}/T_a \tag{14b}$$

Figure 5 shows the variation of the optimum fluid temperature (T_c^*) with the major collector parameters A and B. It varies from about 50°C (122°F) for low performance flat-plate collectors to around 1400°C (2550°F) for high performance concentrators at the given ambient conditions. The optimum temperature is highly sensitive to the heat loss parameter B when B is small (e.g., for high performance collectors), but with less sensitivity as B tends to be larger (e.g., for low performance collectors).

Another interesting result could be reached for the relationship between η_c^* and η_e^* at the optimum fluid temperature T_c^* at large fluid flow rates. The approximate expressions given by Eqs. (12) would yield

$$\eta_c^* \cong \left(A + \frac{B\,T_a}{I}\right)\eta_e^* \tag{15}$$

which means that the maximum overall conversion efficiency will only occur at the intersection point between the collector and reversible engine efficiency curves provided that the quantity $(A + (BT_a/I))$ is approximately unity. The location of the optimum temperature will be lower than the intersection temperature or higher depending on whether the value of $(A + (BT_a/I))$ is larger or smaller than 1, respectively.

The optimum fluid temperature, as shown in Fig. 5, depends on the slope, B, and intersect, A, of the collector efficiency line. Smaller slopes and larger intersections achieve higher overall conversion efficiency and higher optimum temperatures. This explains why high concentration focusing collectors are offering a superior performance compared to low performance non-focusing types.

In the limit, as the parameter A approaches unity and B approaches zero, hypothetically, the optimum temperature T_c^* approaches infinity, the collector efficiency approaches unity, and the overall conversion efficiency approaches the relative efficiency λ as a limiting factor that will never be reached; otherwise, it violates the thermodynamics laws.

B. Sensitivity to the Collector Characteristic Intersect A

Similar procedures can be followed, and it can be shown from Eqs. (8) and (9) that for the parameter A, the overall efficiency sensitivity S_A is

$$S_A = \bar{S}_A = \frac{A}{\eta_c \eta_e}\left(\frac{T_H - T_a}{T_H}\right) \tag{16}$$

Equation (16) also shows that the sensitivity S_A is independent of the relative engine efficiency (λ), and it is always a positive quantity. From thermodynamics principles, it can be proven that the reversible cycle efficiency η_e given by Eq. (3) for a high temperature finite source (varying between T_c and T_H) is always less than the Carnot's expression with the high temperature infinite source (T_H) when both are working with the low temperature infinite sink (T_a). In other words, the quantity $(T_H - T_a)/T_H \eta_e$ is always greater than one. Since the quantity A/η_c is always greater than unity, as evidenced from Eq. (1), the final result is that S_A is always larger than unity at all operating conditions and for any collector type. This gives the collector optical performance a major role in determining the plant overall efficiency. Figure 6 gives a plot of the sensitivity S_A for various collector types. The sensitivity S_A decreases as A increases and/or as B decreases. In the practical region of collector constants where A varies between a minimum of 0.4 to 0.85 maximum, and B varies between, say, a minimum of 0.0001 to 0.0060 kW/m²°C maximum, the sensitivity S_A varies between 1.2 for high performance collectors to 1.9 for low-performance types. In the hypothetical case, where $A \to 1$ and $B \to 0$, the sensitivity S_A approaches 1.

C. Sensitivity to the Collector Characteristic Slope B

The overall efficiency sensitivity S_B can be written using Eqs. (8) and (9) as

$$S_B = \bar{S}_B = \frac{-B(T_c - T_a)(T_H - T_a)}{\eta_c I \cdot \eta_e T_H} \tag{17}$$

Equation (17) shows clearly that S_B is always a negative quantity independent of the power conversion system parameter λ. The negative sign is expected and in agreement with the intuition that the larger the slope of a solar collector, the larger the thermal losses and the lower the overall efficiency will be. No decisive conclusion can be made about whether S_B is larger than one or smaller than one, although the quantity $(T_H - T_a)/T_H\ \eta_e$ is always larger than one as discussed before, but the quantity $B(T_c - T_a)/I\eta_c$ can be either less than or larger than one from Eq. (1). However, the sum (which may have no physical interpretation) of S_A and S_B from Eqs. (16) and (17) is found to be always positive and greater than one:

$$S_A + S_B = \bar{S}_A + \bar{S}_B = \frac{T_H - T_a}{\eta_e T_H} \tag{18}$$

In practice, the quantity $((T_H - T_a)/\eta_e T_H)$ is slightly larger than unity and the sensitivity S_B could be approximated as $(1 - S_A)$.

As a numerical example for the relative magnitudes of S_A and S_B, take the collector constants A and B as 0.8 and 0.0057 kW/m^2°C, respectively, a fluid heat capacity $G_f C_f$ of 0.04 kW/m^2°C, and an optimum inlet fluid temperature of 82.58°C (355.73 K) as given before. The exit fluid temperature T_H^* (from Eq. (4)) will be 94.37°C (367.52 K), the optimum collector and reversible cycle efficiencies become 47.18 and 17.55 percent, respectively, and the sensitivities S_A and S_B are calculated as 1.824 and −0.748. The above shows how the effects of A and B can be quite significant on the overall efficiency, and the designer should always be seeking higher values for A and smaller values for B to improve the performance.

In Fig. 7, a plot is made for the sensitivity S_B at different values of A and B. The absolute value of sensitivity S_B becomes smaller as A increases or B decreases. The limits of S_B for current collectors range from −0.2 (for high performance types) to −0.8 (for low performance types).

D. Sensitivity to Ambient Temperature Variations

The overall efficiency sensitivity, S_{T_a}, to the ambient temperature variations can be derived from Eqs. (8) and (9) using Eqs. (1), (3), (4), (11), and (16) as follows:

$$S_{T_a} = \bar{S}_{T_a} = 1 - S_a - S_{T_c} \tag{19}$$

or at the optimum temperature T_c^*,

$$S_{T_a}^* = \bar{S}_{T_a} = 1 - S_a^*$$

Once more, the sensitivity S_{T_a} is independent of the engine parameter λ. To determine the relative magnitude of S_{T_a}, the numerical values assigned in the last example would yield S_{T_a} equal to −0.824. The negative sign indicates that lowering the ambient temperature will yield an increase in the overall conversion efficiency in spite of the resulting decrease in the collector's efficiency. Figure 8 shows a plot of the sensitivity S_{T_a} at different values of A and B. Numerically, the sensitivities S_{T_a}, $(1 - S_a)$ and S_b are found to be of the same order when Figs. 7 and 8 are compared. Different reference ambient temperatures were found to cause minor changes in S_{T_a} as shown in Fig. 8.

E. Sensitivity to Solar Radiation Intensity

Using Eq. (8), the overall efficiency sensitivity to the solar radiation, I, can be written after some reductions as

$$S_I = \frac{A\,(T_H - T_a)}{\eta_c \eta_e T_H} - 1 \tag{20}$$

It has been shown in Eq. (16) that the quantity $[A(T_H - T_a)/\eta_c\eta_e T_H]$ is always greater than unity; therefore, S_I is always a positive quantity and, in most cases, is less than unity. From Eqs. (16) and (20),

$$S_I = S_A - 1 \tag{21}$$

At this point, it is advantageous to determine the sensitivity $(\bar{S}_I)$ for the net mechanical (or electrical) work generated subject to solar intensity variations. The net work output per unit collector area and the sensitivity, $\bar{S}_I$, can be written using Eqs. (7) and (9) as

$$\bar{S}_I = S_I + 1 = S_A \tag{22}$$

$\bar{S}_I$ is always a positive quantity larger than unity. For instance, in the last numerical example, a 1 percent increase in the solar intensity will cause an increase in the mechanical work output by 1.824 percent and an increase in the overall conversion efficiency by 0.824 percent. Note that for parameters other than solar flux, I, the overall efficiency sensitivity, S, is identical to the net work sensitivity, $\bar{S}$.

Figure 9 is a plot of the sensitivity S_I at different values of A and B. Two reference values for I were tried (1 kW/m^2 and 0.5 kW/m^2), and the results show that the larger the solar flux variation, the larger the sensitivity S_I and $\bar{S}_I$ will be. However, larger values of A and smaller values of B tend to reduce the sensitivity S_I.

The results obtained from the above steady state analysis are in agreement with the results obtained in Refs. 1 and 2, using a dynamic radiation model composed of sinusoids. Values of $\bar{S}_I$ between 1.62 and 1.9 at one sun (1 kW/m^2 peak) were obtained in Ref. 1 for the fast-response NASA-Honeywell collector (A = 0.713, B = 0.0029 kW/m^2°C to 0.0036 kW/m^2°C, Ref. 7) and $\bar{S}_I$ between 1.61 and 1.70 for the slow response Owens-Illinois collector (A = 0.45 and B = 0.0014 kW/m^2°C, Ref. 7). A comparison with Fig. 9 shows the close behavior of the system response to the solar flux radiation between the present quasi-steady state and the dynamic transient model.

F. Sensitivity to the Collector Fluid Heat Capacity

The heat capacity of the collector fluid, $G_f C_f$, is one of the parameters that can alter the exit fluid temperature, which in turn affects the engine's performance. The sensitivity S_G is determined from Eqs. (8) and (9) at the reference state as

$$\bar{S}_G = S_G = \frac{G_f C_f}{\eta_c} \frac{\partial \eta_c}{\partial (G_f C_f)} + \frac{G_f C_f}{\eta_e} \frac{\partial \eta_e}{\partial (G_f C_f)} \quad (23)$$

For almost all solar collectors, the constants A and B in the efficiency expression, Eq. (1), can be subdivided to be in the form:

$$\eta_c = F \left[A' - B' \left(\frac{T_c - T_a}{I} \right) \right] \quad (24)$$

where F is a dimensionless flow factor dependent on the flow characteristics and

$$\left. \begin{aligned} A &= A'F \\ B &= B'F \end{aligned} \right\} \quad (25)$$

Usually, the constants A and B have, at most, a very weak dependence on the flow characteristics. The first term in the right-hand side of Eq. (23), namely, $(G_f C_f / \eta_c)$ $(\partial \eta_c / \partial G_f C_f)$ will then be reduced to $G_f C_f / F \cdot \partial F / \partial G_f C_f$. The latter is always positive since increasing the flow rate improves the collector's efficiency in turn. On the other hand, the second term in the right-hand side of Eq. (23) can be written using Eqs. (3) and (4) as

$$\frac{G_f C_f}{\eta_e} \frac{\partial \eta_e}{\partial G_f C_f} = 1 - \frac{T_H - T_a}{\eta_e T_H} = 1 - (S_A + S_B) \quad (26)$$

which is usually a very small negative quantity as shown by Eq. (18). If the variations of the flow factor F with the heat capacity $G_f C_f$ is small, such that it can be neglected, then Eq. (26) can be used as a first approximation to the sensitivity S_G in comparison with other sensitivity expressions. In reality, S_G will be somewhat smaller than the approximate form given by Eq. (26) due to the opposing presence of F variations. Figure 10 is a plot of the sensitivity S_G as approximated by Eq. (26) at different values of A, B, and reference fluid heat flux $G_f C_f$. The effect of the parameter A is negligible, but the effect of B is quite significant. At the reference value of $G_f C_f$ of 0.04 kW/m^2°C, the sensitivity S_G varies between −0.001 (high performance collectors, $B \simeq$ 0.0001) to −0.08 (for low performance collectors, B = 0.0060 kW/m°C). Changing the flow heat capacity has caused a proportional change in the sensitivity S_G as shown in Fig. 10. Although the sensitivity S_G tails the list of the whole parameters discussed above, it could have a significant degradation effect on the overall performance. In practice, the choice of the operating flow rate is based on a trade-off between the system efficiency and pumping power. Reference 15 gives a practical range of $G_f C_f$ for flat plate collectors to be from 24.4 kg/h · m^2 (~5 lb/h · ft^2) to 97.7 kg/h · m^2 (~20 lb/h · ft^2) with a recommended value of about 48.8 kg/h · m^2 (~10 lb/h · ft^2). These flow values, however, could be used for other solar power plants as a starting point in the design.

G. Sensitivity to the Conversion Relative Efficiency

The engine-transmission parameter λ has a direct one-to-one correspondence effect on the overall plant efficiency and work output. The sensitivity S_λ (or $\bar{S}_\lambda$), as deduced from Eq. (9), is equal to 1 keeping all other parameters unchanged.

V. Summary

Discrepancies between design data and actual performance are expected to take place in the design and operation of future solar thermal-electric power systems, as in the case of any other system. Seven major design parameters were identified and their weight on performance variations were analyzed and estimated as a first phase of the study excluding the economic factors. The parameters studied were: (1) fluid temperature entering the energy collection subsystem, (2) optical characteristics of the energy collection subsystem, (3) thermal loss characteristics of the energy collection subsystem, (4) ambient temperature, (5) incident solar flux, (6) heat capacity of working fluid, and (7) relative efficiency of energy conversion-transmission subsystems. An analytical model for all solar thermal-electric plants was laid out to enable the sensitivity expressions to be derived and evaluated in a general manner. The total effect on the plant performance is summed, as given in Eq. (10). The performance sensitivity to the inlet fluid temperature was found changing from $+\infty$ at the ambient temperature to $-\infty$ at the collector's limiting temperature $\bar{T}_c$, with a zero sensitivity at the optimum fluid temperature T_c^*. The temperature T_c^* is usually taken as the plant design point since it corresponds to the maximum overall conversion efficiency.

Second, the sensitivity S_A to the optical characteristic parameter A was found to always be positive, greater than unity (1.2-1.9), and independent of the relative power cycle efficiency, λ. Third, the sensitivity S_B to the thermal losses parameter (B) was found to always be negative ($-0.2 \rightarrow -0.8$) independent of λ and have the same order of magnitude as the sensitivity to ambient temperature (S_{T_a}). Fourth, the sensitivity S_{T_a} was found to always be negative, independent of λ, and, in all present systems, less than one. Fifth, the variations of the solar flux I will result in sensitivities always larger than one (between 1.2-1.9) for the net work output. Finally, the least sensitivity of performance resulted from the fluid heat flux variations. Although increasing the fluid rate in the collection subsystem would improve the heat transfer coefficients and increase the harnessed energy, the negative impact of reducing the exit temperature from the collection subsystem and the resulting decrease of the power cycle efficiency outweigh the benefit. All of the sensitivity expressions need to be substituted in Eq. (10) to determine the dynamic analysis of the system when it operates at off-design conditions.

This first-phase parameterization study has not only helped in shedding some light onto some major design variables which need to be accurately evaluated and closely adhered to during operation, but the effect of the probabilistic weather changes on performance is also quantified by some limiting values. The results would be most helpful in guiding the preliminary design stages, the future plant specifications, and the second phase of the study indicating the effects on unit energy costs at the bus bar.

Acknowledgment

The authors would like to acknowledge Phillip Moynihan, Manager of the Systems Engineering and Development Task, and Toshio Fujita, Manager of the Advanced Systems Identification Task, and both of the Solar Power System Projects in the Energy Technology and Application office (ET&A), who provided a number of invaluable suggestions in the present study.

References

1. Hamilton, C. L., "Dynamic Modeling and Sensitivity Analysis of Solar Thermal Energy Conversion Systems," *Deep Space Network Progress Report 42-41*, pp. 226-232, Jet Propulsion Laboratory, Pasadena, CA, Oct. 1977.

2. Reid, M. S., Hamilton, C. L., and Hester, O. V., "The Engineering Analysis of Solar Radiation," *International Journal of Policy Analysis and Information Systems*, Vol. 2, No. 1, pp. 187-217, July 1978.

3. Simon, F., *Solar Collector Performance Evaluation with the NASA-Lewis Solar-Simulator Results for an All-Glass-Evacuated Tubular Selectively-Coated Collector with a Diffuse Reflector*, NASA TMX-71695, NASA-Lewis Research Center, Cleveland, Ohio, April 1, 1975.

4. Ari Rabl, *Optical and Thermal Properties of Compound Parabolic Concentrators*, Argonne National Lab, Argonne, Illinois, February 1975.

5. *Performance Study of the Compound Parabolic Concentrator Solar Collector*, report prepared by Environmental Consulting Services, Inc., Boulder, Colorado, for the Argonne National Laboratory, September 1974.

6. *Corning Tubular Evacuated Collector*, Corning Glass Works, Lighting Products Division, Corning, New York, January 1975.

7. Simon, F., *Flat-Plate Solar-Collector Performance Evaluation with a Solar Simulator as a Basis for Collector Selection and Performance Prediction*, NASA TMX-71793, NASA-Lewis Research Center, Cleveland, Ohio.

8. Kleinkauf, W., Kohne, R., Lindner, F., and Simon, M., "A Solar Power Plant in the 10 KWe Range with Focusing Collectors," *International Aerospace Abstracts*, Technical Information Service of AIAA, paper No. A76-45995, American Institute of Astronautics and Aeronautics, New York, New York, March 1976.

9. Ramsey, J. W., Sparrow, E. M., and Ecker, R. R. G., "Solar Thermal Electric Power Generation Using a System of Distributed Parabolic Through Collectors," *International Aerospace Abstracts*, Technical Information Service AIAA, paper No. A75-47511, American Institute of Astronautics and Aeronautics, New York, New York, August 1975.

10. *Solar Energy Program Semiannual Review Report*, Sandia Laboratories, Albuquerque, New Mexico, July 1976.

11. *Northrop Collector*, Northrup Incorporated, Hutchins, Texas, 1975.

12. Shimada, K., and Swerdling, M., *Terrestrial Solar Thermonic Energy Conversion Systems Concept*, Technical Memorandum 33-744, Jet Propulsion Laboratory, Pasadena, CA, November 1975.

13. Lansing, F. L., and Dorman, J., "High Efficiency Solar Concentrator," *Deep Space Network Progress Report 42-35*, pp. 99-109, Jet Propulsion Laboratory, Pasadena, CA, October 1976.

14. Anderson, D. E., and Stickley, R. A., "A Line Focus Segmented Mirror Concentrator," *Optics in Solar Energy Utilization II, SPIE*, Vol. 85, pp. 121-127, 1976.

15. Hewitt, H. C., and Griggs, E. I., "Optimal Mass Flow Rates Through Flat Plate Solar Collector Panels," ASME publication 76-WA/Sol-19, presented at ASME winter annual meeting, New York, N.Y., Dec. 1976.

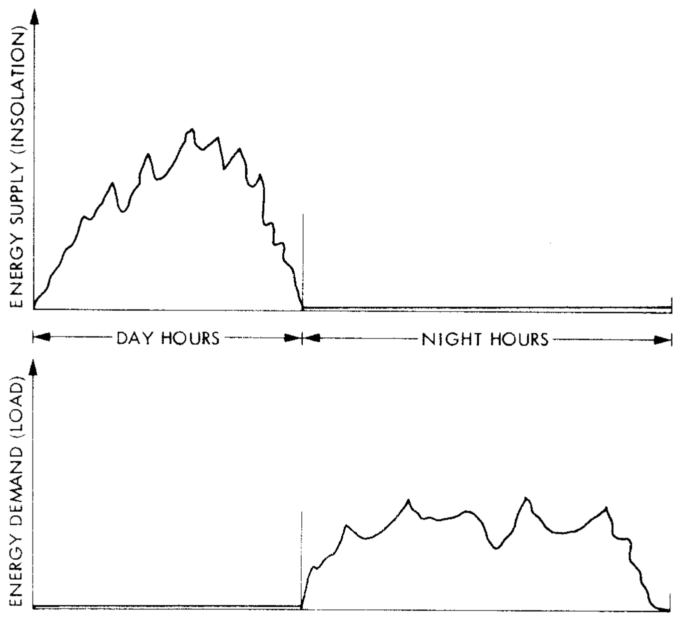

Fig. 1. Insolation and load profile

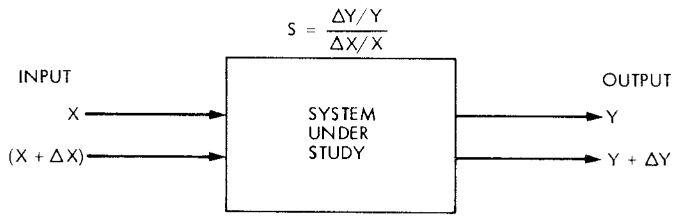

Fig. 3. Sensitivity definition

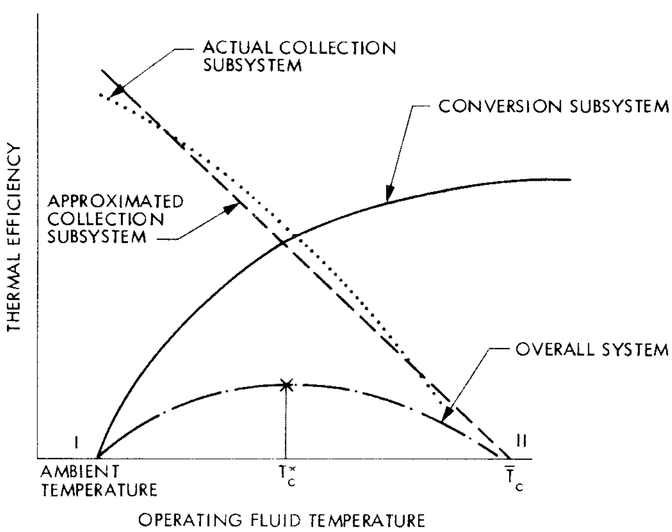

Fig. 2. Efficiency trends for collection and conversion subsystem

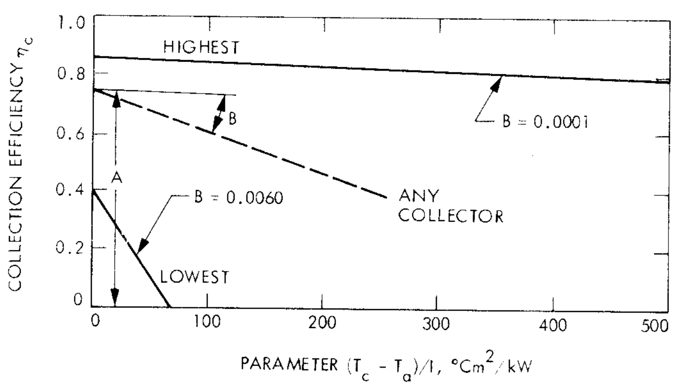

Fig. 4. Lowest and highest performance of current solar collector designs

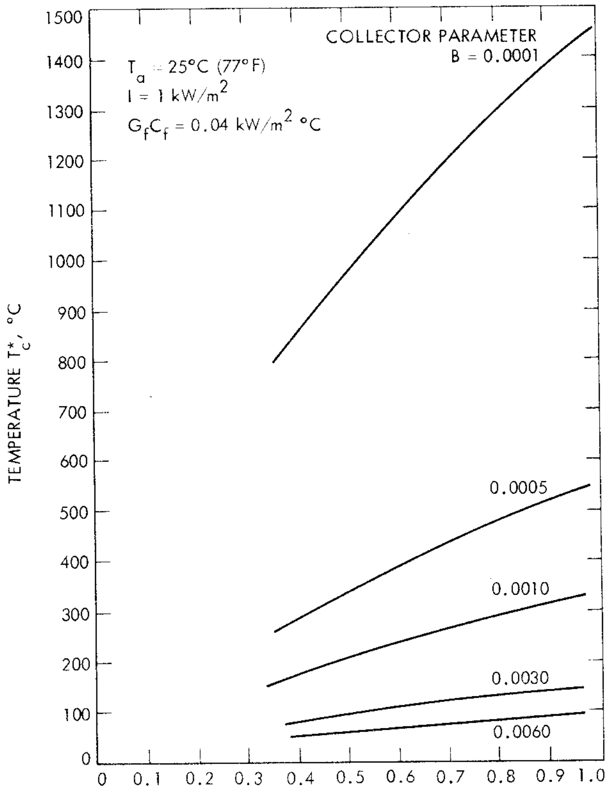

Fig. 5. Optimum inlet fluid temperature to collector for various designs

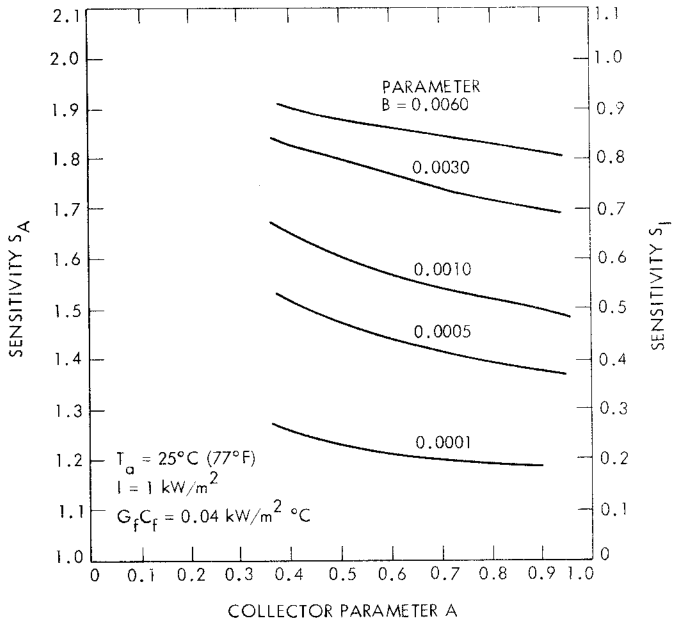

Fig. 6. Efficiency sensitivity S_A at optimum fluid temperature

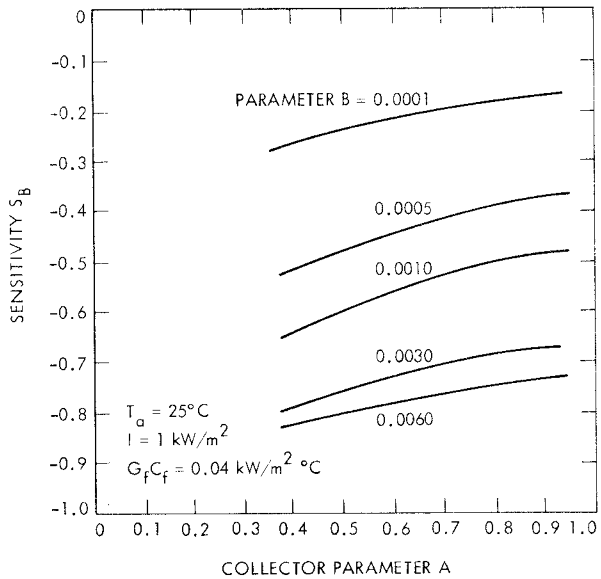

Fig. 7. Sensitivity S_B at optimum design point of various collector designs

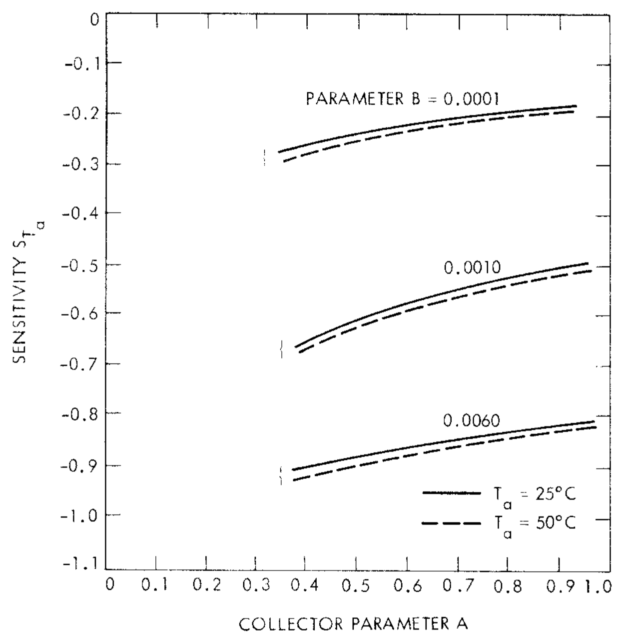

Fig. 8. Sensitivity S_{T_a} at different temperature and optimum design point

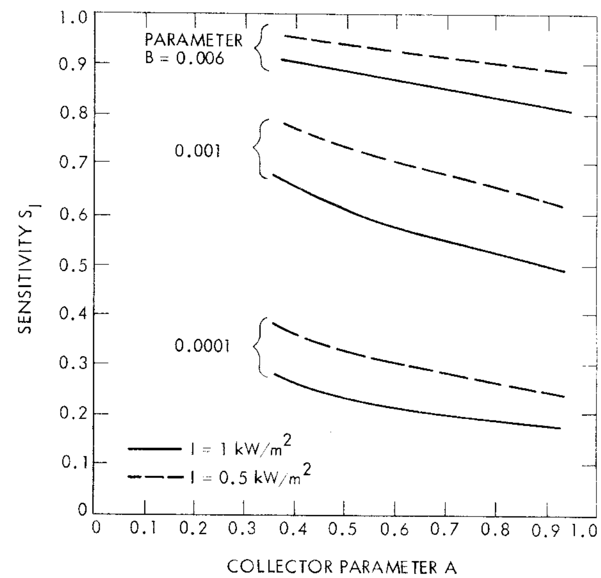

Fig. 9. Sensitivity S_I at various solar intensities and for different designs

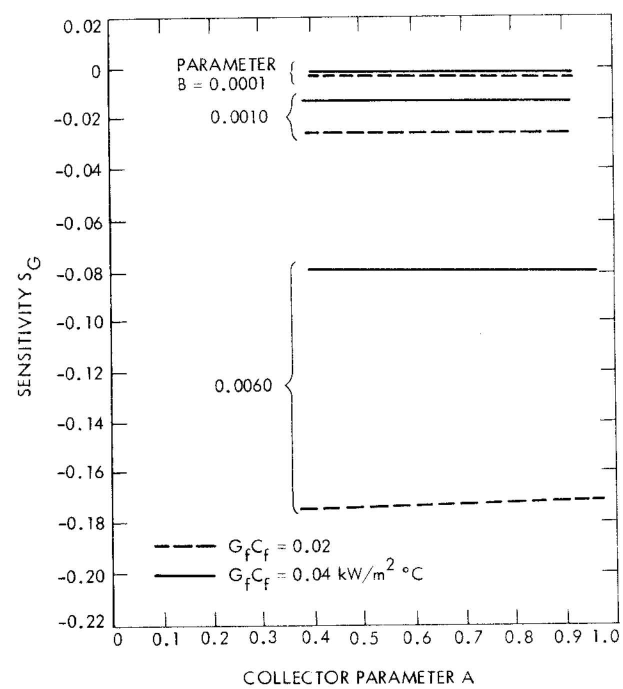

Fig. 10. Sensitivity S_G at different fluid heat flux and for different optimum designs